Clinical & Experimental Immunology
The Journal of Translational Immunology

Clinical and Experimental Immunology ORIGINAL ARTICLE doi: 10.1111/cei.13422

Low-dose IL-2 induces CD56^{bright} NK regulation of T cells via NKp44 and NKp46

S. L. McQuaid,*† S. T. Loughran,*‡,1 P. A. Power,*§,1 P. Maguire,*¶ A. Szczygiel* and P. A. Johnson *

*Viral Immunology Laboratory, School of Nursing, Psychotherapy and Community Health, Dublin City University, †Mason Technology Ltd, Dublin, ‡Department of Applied Science, Dundalk Institute of Technology, Dundalk, §Technological University Dublin, and ¶School of Biotechnology, Dublin City University, Dublin, Ireland

Accepted for publication 12 January 2020
Correspondence: P. Johnson, Viral Immunology Laboratory, School of Nursing, Psychotherapy and Community Health, Dublin City University, Glasnevin, Dublin 9, Ireland.
E-mail: patricia.johnson@dcu.ie

[1]These authors contributed equally to this study.

Summary

Low-dose interleukin (IL)-2 has shown clinical benefits in patients with autoimmune and inflammatory diseases. Both regulatory T cells (T_{regs}) and natural killer (NK) cells are increased in response to low-dose IL-2 immunotherapy. The role of regulatory T cells in autoimmune diseases has been extensively studied; however, NK cells have not been as thoroughly explored. It has not been well reported whether the increase in NK cells is purely an epiphenomenon or carries actual benefits for patients with autoimmune diseases. We demonstrate that low-dose IL-2 expands the primary human CD56^{bright} NK cells resulting in a contact-dependent cell cycle arrest of effector T cells (T_{effs}) via retention of the cycle inhibitor p21. We further show that NK cells respond via IL-2R-β, which has been shown to be significant for immunity by regulating T cell expansion. Moreover, we demonstrate that blocking NK receptors NKp44 and NKp46 but not NKp30 could abrogate the regulation of proliferation associated with low-dose IL-2. The increase in NK cells was also accompanied by an increase in T_{reg} cells, which is dependent on the presence of CD56^{bright} NK cells. These results not only heighten the importance of NK cells in low-dose IL-2 therapy but also identify key human NK targets, which may provide further insights into the therapeutic mechanisms of low-dose IL-2 in autoimmunity.

Keywords: autoimmunity, CD56^{bright} NK, low-dose IL-2, NK cells, NKp44, regulatory T cells

Introduction

Low-dose IL-2 has shown clinical benefits in inflammatory conditions such as hepatitis C virus (HCV)-induced vasculitis, chronic graft-*versus*-host disease (GVHD) and type I diabetes (T1D) [1–3]. Both T regulatory cells (T_{regs}) and natural killer (NK) cells are consistently increased in response to this cytokine in patients. While a role for T_{regs} has been established, the involvement of NK cells has been understudied [1–9].

Two main subtypes of NK cells have been identified in humans based on their expression of the surface marker CD56: CD56^{bright} and CD56^{dim}. It has been widely reported that CD56^{dim} NK cells act cytotoxically on infected or tumour cells, while CD56^{bright} NK cells are considered the more regulatory subset, due to their release of regulatory cytokines [10,11]. However, more recent studies have shown that CD56^{bright} marker does not unanimously define NK cells with the strongest cytokine-producing capabilities and that these NK cell subsets may also display greater degranulation and killing in response to tumour cell targets [12].

Recent reports involving NK cells have identified regulatory properties which could contribute to the improved effects in autoimmune and inflammatory conditions. Patients with active forms of multiple sclerosis (MS) receiving daclizumab, a humanized monoclonal antibody to IL-2 receptor alpha (IL-2Rα), demonstrated a significant expansion of CD56^{bright} NK cells *in vivo* [13]. This was highly correlated with a profound treatment response resulting in a reduction in brain inflammatory activity and a marked reduction in the number of magnetic resonance imaging (MRI) gadolinium (Gd)-enhancing lesions [13]. Moreover, low levels of CD56^{bright} NK cells have been associated with chronic GVHD, and

an early increase of CD56^{bright} NK cells is considered a predictor of response to extracorporeal photopheresis (ECP) treatment for GVHD [14–18]. In addition, a recent study demonstrated that IL-2 treatment combined with ECP led to enhanced CD56^{bright} NK cells compared with ECP alone [19]. Other studies have shown that patients with chronic GVHD displayed low expression of the NK activation receptor, NKG2D [20]. In addition, patients with relapsing–remitting MS have shown that NK cell activity drops prior to clinical relapse and that clinical remission is preceded by an increase in NK cell activity [21]. Further research also found that patients with autoimmune diseases such as MS and rheumatoid arthritis (RA) have fewer blood levels of NK cells and that NK cells isolated from patients with MS have impaired effector function in addition to decreased frequency of NK cells [22,23]. These studies suggest that NK cells could potentially be disease-controlling in autoimmune and inflammatory diseases. In addition to these studies, we have identified that HPIV3 infection of human monocytes induces low levels of IL-2 in human T cells, resulting in expansion of CD56^{bright} NK cells and subsequent CD56^{bright} NK-dependent inhibition of T cell proliferation [24]. Follow-on studies identified that the haemagglutinin-neuraminidase (HN) component of the virus interacts with CD56^{bright} NK cells via NK receptors NKp44 and NKp46 to induce cell cycle arrest of T cells. This arrest could be rescued by increasing IL-2 levels [25]. These findings suggest that HPIV3 induces CD56^{bright} NK regulation of T cell proliferation in an IL-2-dependent manner [25]. This led us to speculate if this method of NK regulation could be a factor in the clinical utility of low-dose IL-2 in human inflammatory and autoimmune conditions.

The findings presented in this study demonstrate that within primary human peripheral blood mononuclear cells (PBMCs), CD56^{bright} NK cells expand and cause T cell cycle arrest at low IL-2 concentrations, contract and allow T cell proliferation at intermediate IL-2 concentrations and expand again at high IL-2 concentrations, causing T cell death. In addition, further investigations reveal that consistent with cell cycle arrest, the cell cycle inhibitor p21 is retained in T cells in the presence but not the absence of NK cells at low-dose IL-2. Subsequent studies suggest that NK cells are activated via IL-2Rβ to drive regulation of T cell expansion at low- and high-dose IL-2. In addition, we provide evidence that regulation of T effector (T_{eff}) cell proliferation by NK cells is contact-dependent and mediated by NKp44 and NKp46. Interestingly, while suppressing the overall T cell population, NK cells appear to boost T_{reg} numbers at low-dose IL-2. Strikingly, the T_{reg} population was unable to significantly increase in response to IL-2 in the absence of CD56^{bright} NK cells. This study supports a role for human NK cells in the beneficial effects of low-dose IL-2 therapy in human autoimmune conditions.

Methods

Cell culture was carried out in accordance with the Safety and Health Policy of Dublin City University and, where appropriate, with the notification of the Health and Safety Authority.

Separation of PBMCs

Buffy coats from healthy donors were obtained from the Irish Blood Transfusion Service (at St James' Hospital, Dublin). The peripheral venous blood (approximately 50 ml) was mixed with 5 ml of a 5% solution of ethylenediamine tetraacetic acid (EDTA) (Sigma-Aldrich, Ireland) and diluted 1 : 3 with Hanks' balanced salt solution (HBSS) (Gibco, UK) containing 1% fetal calf serum (FCS) (Gibco, UK) and 10 μM HEPES buffer (Gibco UK). This diluted blood was layered onto 14 ml of density gradient medium Lymphoprep^{TM} (Axis-Shield, Oslo, Norway) and centrifuged at 400 ***g*** for 25 min (with accelerator and break switched off). With blood components separated according to density, the buffy coat layer was removed, and cells were washed twice with 10 ml of complete Roswell Park Memorial Institute (cRPMI)-1640 medium (supplemented with 10% FCS, 10 mM HEPES, 2 mM L-glutamate, 100 U penicillin (Gibco, UK)/ml and 100 μg streptomycin (Gibco, UK)/ml). Finally, cells were filtered through a 40-μM filter and diluted to the required cell number per ml.

Separation, purification and depletion of cell subsets from PBMCs using microbead separation

Cells were purified from PBMCs using magnetic microbeads by MACS (Miltenyi Biotec, Woking, UK). PBMCs were resuspended in MACs buffer [sterile phosphate-buffered saline (PBS) supplemented with 0·5% bovine serum albumin (BSA) and 2 μM EDTA] and incubated with target-cell specific antibodies conjugated to magnetic microbeads, according to the manufacturer's instructions. Following incubation, cells were washed with magnetic-activated cell sorting (MACs) buffer. For positive selection of CD56^{+} or CD3^{+} cells, cell suspension was applied to an LS column attached to a magnet. The column was washed three times with 3 ml of MACs buffer. The positively labelled cells were flushed out of the column with a plunger in the absence of magnetic force. The initial 'flow-through' and wash step were used as the CD56^{+} cell-depleted fraction. For isolation of CD56^{bright} NKs (CD56^{+}CD16^{-}), CD56^{dim} NKs (CD56^{+}CD16^{+}) or T_{regs} (CD4^{+}CD25^{+}), specific cell purification kits were used (Miltenyi Biotec). Purities were determined by flow cytometry using a FACSCalibur^{TM} Flow

Cytometer (BD Biosciences, Wokingham, UK) and Cyflogic software (CyFlo, Turku, Finland) in conjunction with surface marker staining and were routinely ≥ 97%. Surface marker staining was performed with specific antibodies (eBioscience, Altrincham, UK), according to the manufacturer's instructions.

Cell culture and IL-2 stimulation

Mixed lymphocytes (MLs) or $CD56^+$ cell-depleted MLs were cultured at 1×10^6 cells/ml on a 24-well plate. MLs were stimulated with a range of concentrations of IL-2 (Miltenyi Biotec). For this, doubling dilutions of IL-2 were carried out from 50 to 0·781 ng/ml IL-2 using cell culture media as diluent prior to stimulation. Co-culture of $CD3^+$ plus $CD56^{bright+}$ cell and $CD3^+$ and $CD56^{dim}$ subsets was carried out at 100 : 1 and 10 : 1 ratios, respectively. This represents the physiological ratios of these cells in the human periphery. Stimulated cells were cultured for 5 days at 37°C.

Cell cycle and apoptosis assay

After 5 days' incubation, cells were pelleted and washed twice with flow cytometry buffer (BD Pharmingen, Wokingham, UK). For cell cycle analysis, cells were stained with propidium iodide (PI) (BD Pharmingen). Cells were also labelled with allophycocyanin (APC)-conjugated antibody to CD3. Upon acquisition, $CD3^+$ cells were gated for and the percentage of these cells in the G0/G1 phase of cell cycle determined. For analysis of cell death, cells were stained with fluorescein isothiocyanate (FITC) annexin V and PI using the FITC annexin V Apoptosis Detection Kit I (BD Pharmingen), according to the manufacturer's protocol, and were also labelled with APC-conjugated antibody to CD3. FACSCalibur™ Flow Cytometer (BD Biosciences) and Cyflogic software (CyFlo) were used to analyse the level of apoptosis in each sample.

Inhibitor protein and perforin determination

MLs were cultured under various conditions and harvested. Cells were collected, washed with PBS and the cell pellet was lysed in cell extraction buffer [10 mM TRIS, pH 7.4, 100 mM NaCl, 1 mM EDTA, 1 mM ethylene glycol teraacetic acid (EGTA), 1 mM NaF, 20 mM $Na_4P_2O_7$, 2 mM Na_3VO_4, 1% Triton X-100, 10% glycerol, 0·1% sodium dodecyl sulphide (SDS), 0·5% deoxycholate, 1 mM PMSF, 10% protease inhibitor cocktail (Sigma-Aldrich, Poole, UK)] for 30 min on ice, and vortexed at 10-min intervals. The cell extract was centrifuged (14 000 ***g***) for 10 min at 4°C. Inhibitor protein expression was determined by p21 and p27-specific enzyme-linked immunosorbent assay (ELISA) kits (Invitrogen, Inchinnan, Scotland, UK), according to the recommended protocol. For perforin determination, cells were harvested, permeabilized and stained using anti-CD56-FITC and anti-perforin phycoerythrin (PE) antibodies (eBioscience) and analysed by flow cytometry using a FACSCalibur™ Flow Cytometer (BD Biosciences) and Cyflogic software (CyFlo). Quadrant gates were set according to isotype controls. The percentage of $CD56^+$perforin$^+$ cells was expressed as a percentage of total $CD56^+$ cells.

Carboxyfluorescein succinimidyl ester (CFSE) incorporation

CFSE staining was performed for $CD56^{bright}$ NK cells, $CD56^{dim}$ NK cells, $CD3^+$ cells or T_{regs}. This assay is used as a method for tracking cell proliferation. Cells were centrifuged and resuspended in a solution of 0·1% BSA in PBS at a final concentration of 1×10^6 cells/ml. A 5-mM vol. of stock CFSE solution was added to 1×10^6 cells to yield a final working concentration of 10 μM. Cells were incubated at 37°C for 10 min. Staining was then quenched by the addition of 5 vol. ice-cold culture media to the cells. Cells were incubated for 5 min on ice and then pelleted by centrifugation. Cells were washed three times in fresh culture media. Upon acquisition by flow cytometry, the peak of cells emitting low levels of CFSE was gated for analysis to determine the percentage of proliferated cells.

IL-2 receptor blocking experiments

$CD3^+CD56^-$ T cells were isolated and labelled with CFSE as above. Purified monoclonal antibodies to both IL-2Rα and IL-2Rβ [R&D Systems, Abingdon, UK; species of origin: mouse immunoglobulin (Ig)G_1] were used to block IL-2Rα, IL-2Rβ or both receptors (with isotype-matched monoclonal antibodies) on purified autologous $CD56^{bright}$ NK and $CD56^{dim}$ cells prior to co-culture and stimulation with IL-2. A concentration of 1 μg/ml was used per 1-ml culture well of cells.

Transwell co-cultures

Transwell inserts function in separating cell types, allowing cytokines to pass between them, but preventing cell–cell contact. Beneath the insert in the lower chamber, 1×10^6 $CD3^+$ cells were cultured. $CD56^+$ cells were cultured with IL-2 in the upper chamber of a 0·2 μM pore insert (Nunc, Lougborough, UK) in the appropriate wells of a 24-well plate. Co-cultures were incubated for 5 days and then analysed as required.

Natural cytotoxicity receptor (NCR) blocking experiments

For receptor blocking, NK cells were cultured with Leaf™ purified A-NKp30, A-NKp44 or A-NKp46 antibodies (Medical Supply Company, Dublin, UK; species of origin: mouse $IgG_1\kappa$) prior to IL-2 stimulation and co-culture. These antibodies have been shown to block these receptors in solution (Medical Supply Company). A-NKp30 served as a negative control, which highlighted no non-specific effects. A concentration

of 1 μg of these antibodies was added to the cell culture media per 1 × 10^6 NK cells/MLs.

Determining T cell subset percentages

Multi-colour detection-kits were used for detecting the percentage of T_{regs} [$CD4^+CD25^+$forkhead box P3($Foxp3^+$), T helper type 1 (Th1) ($CD3^+Tbet^+IFN\gamma^+$)] or Th17 ($CD3^+IL\text{-}17^+IL\text{-}23^+IL\text{-}22^+$) cells, according to the manufacturer's protocols (R&D Systems). Additionally, cells were stained with antibodies for CD3 and CD45RO for determining memory T cell levels, or CD3 and CD8 for detecting the percentage of $CD8^+$ T cells. These subsets were expressed as a percentage of total MLs upon acquisition.

Statistics

Cyflogic and FACSCalibur software were used for FACs analysis, and plots were created using GraphPad Prism version 6.0 for windows (GraphPad Software, Oxford, UK). Statistical analyses were performed using GraphPad Prism version 6.0 and Newman–Keuls one-way analysis of variance (ANOVA): $^*P < 0{\cdot}05$; $^{**}P < 0{\cdot}01$; $^{***}P < 0{\cdot}001$.

Results

We assessed the level of T cell cycling and apoptosis at various IL-2 concentrations in primary total lymphocytes, and $CD56^+$ NK cell-depleted lymphocytes isolated from healthy human blood donors. Gating for $CD3^+$-labelled cells, the percentage of T cells retained in the G0/G1 phase of cell cycle, was determined. At low IL-2, increased percentages of T cells were retained in the G0/G1 phase of cell cycle and at high IL-2, $CD3^+$ T cells underwent increased levels of apoptosis. These effects were abrogated when $CD56^+$ NK cells were depleted from the cultures (Fig. 1a–f). These results suggest a control mechanism whereby T cells are

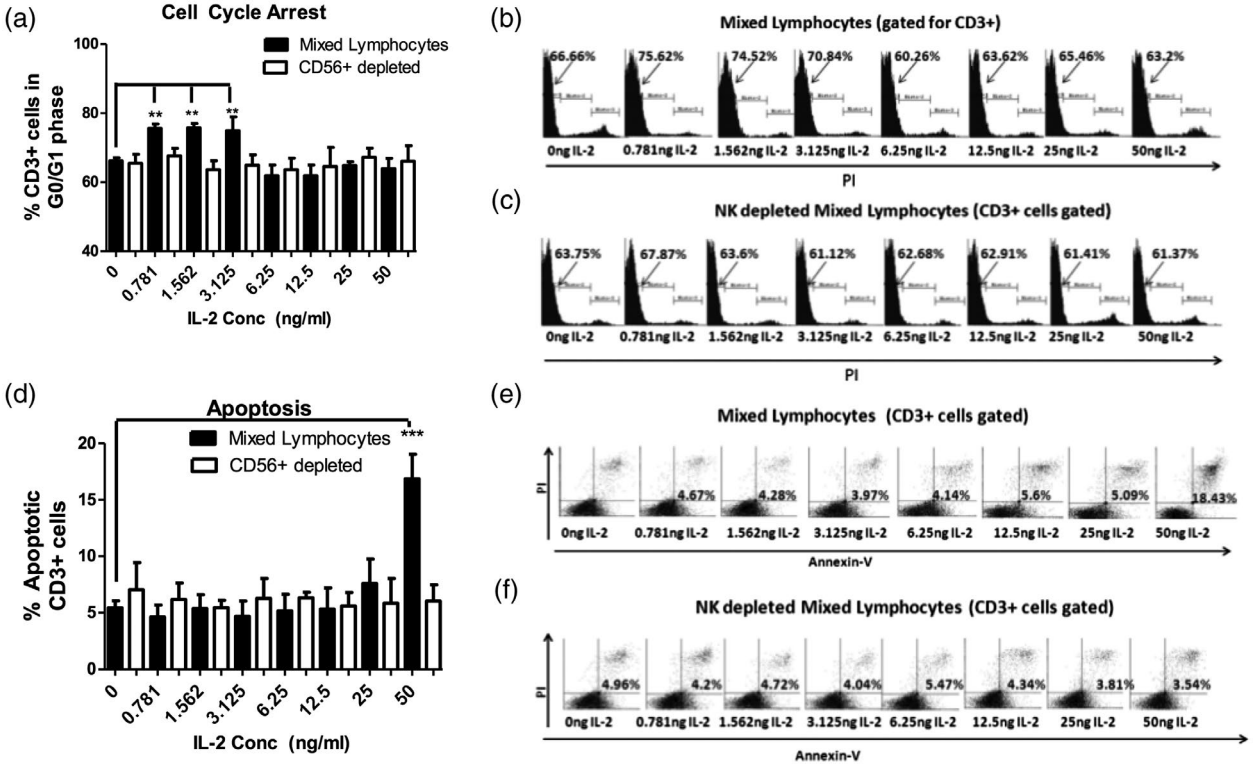

Fig. 1. $CD56^+$ natural killer (NK) cells induce cell cycle arrest at low-dose interleukin (IL)-2 and apoptosis at high-dose IL-2 in autologous T cell populations. Cell cycle (a–c) and apoptotic (d–f) responses of $CD3^+$ cells in response to IL-2 concentrations, in the presence or absence of $CD56^+$ cells, were analysed by flow cytometry. Mixed lymphocytes (MLs) or $CD56^+$-depleted MLs were stimulated with IL-2 (0–50 ng) concentrations for 5 days. After incubation cells were stained with an allophycocyanin (APC)-labelled anti-human CD3 antibody. Cell cycle status ($CD3^+$ gated) was determined by propidium iodide (PI) staining (a–c), while the level of cell death ($CD3^+$ gated) was assessed by PI and annexin V staining (d–f). Bar charts for cell cycle (a) and apoptotic (d) data display normalized results ($n = 3$ donors), with experiments from each donor carried out in triplicate. Values are expressed as mean percentage + standard error of the mean (s.e.m.). Flow cell cycle histograms (b,c) represent a single data set from one donor (of $n = 3$), with relevant markers for the G0/G1, S and G2 phases of cell cycle, and the percentage of $CD3^+$ gated cells in the G0/G1 phase displayed for MLs (b) or $CD56^+$ depleted MLs (c) stimulated with IL-2. Similarly, apoptotic dot-plots (e,f) represent a single data set from one donor (of $n = 3$), with the percentage of annexin V^+ and PI^+ ($CD3^+$ gated) cells (upper right quadrant) displayed. Significance was determined using Newman–Keuls one-way analysis of variance (ANOVA) and is compared to the media sample of the same data set; $^{**}P \leq 0{\cdot}01$, $^{***}P \leq 0{\cdot}001$.

'restrained' in cell cycle arrest by NK cells at low IL-2 and are eliminated by apoptosis at high IL-2.

To elucidate the mechanism by which NK cells may contribute to the arrest of T cell proliferation, we examined other aspects of cell cycle regulation in a further set of donors with or without the presence of NK cells. The progression of T cells from G0/G1 to S phase of the cell cycle is controlled by the activity of cyclins that are tightly regulated by inhibitor proteins such as p27 and p21 [26]. These inhibitors bind to cyclin–CKD complexes and induce cell cycle arrest. To determine the molecular basis of NK cell-induced G0/G1 arrest of T cells in response to IL-2, we examined the status of these cell cycle regulatory proteins in responses to IL-2 with or without the presence of NK cells. Significant increases in the expression of the inhibitor p21 in mixed lymphocytes were observed at low-dose IL-2 when NK cells are present, but not when they are removed from the lymphocyte populations (Fig. 2a). There was an overall increase in p27 in the presence but not absence of NKs; however, this increase was not significant and not related to the different doses of IL-2 (Fig. 2b). To further establish a functional explanation for NK-related increased apoptosis at high-dose IL-2, we examined the levels of perforin in NK cells in response to increasing doses of IL-2. Perforin is a membrane-disrupting protein which works together with a family of structurally related serine proteases (granzymes) to induce apoptosis of the target cell [27]. We observe that cells co-stained for CD56 and perforin in the mixed lymphocyte cultures demonstrated a significant increase in perforin at high-dose IL-2, with increased apoptosis detected at the highest level of IL-2 and perforin (Fig. 2c).

We wished to establish if NK cells inhibit actual proliferation of $CD3^+$ T cell numbers and to identify if decreased proliferation can be attributed to a particular subset of NKs. From a further set of human donors, we isolated $CD3^+CD56^-$ T cells which were subsequently labelled with CFSE. CFSE incorporation is an effective

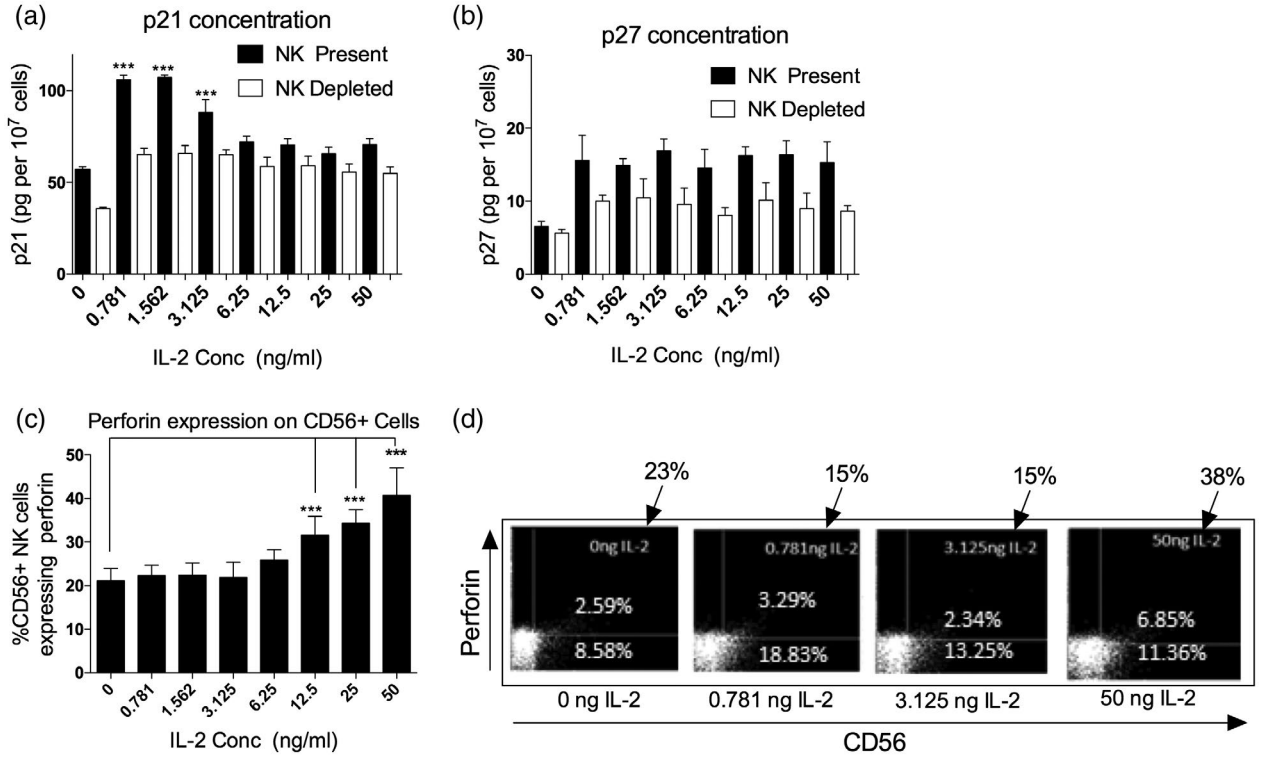

Fig. 2. Cell cycle (G0/G1) arrest of T cells by natural killer (NK) cells correlates with increased p21 expression in mixed lymphocytes (MLs) and apoptosis is accompanied by increasing levels of perforin in NK cells at high-dose interleukin (IL)-2. (a,b) MLs or $CD56^+$ depleted MLs were stimulated with IL-2 (0–50 ng) concentrations for 5 days. (a) The expression of p21 cell cycle regulatory proteins in MLs in response to IL-2 was examined with or without NK cells present by p21 enzyme-linked immunosorbent assay (ELISA). (b) The expression of p27 cell cycle regulatory proteins in MLs in response to IL-2 was examined with or without NK cells present by p27 ELISA. (c) Freshly isolated MLs were stimulated with various IL-2 concentrations. Upon harvest at day 5, cells were stained with fluorescent conjugated antibodies to both perforin and CD56 and analysed by flow cytometry. (c) Perforin expression by NK cells was examined in response to increasing doses of IL-2. When acquired, the percentage of $CD56^+$ $perforin^+$ cells (upper right quadrant) were expressed as a percentage of total $CD56^+$ cells (upper + lower right quadrants). Results represent normalized data ($n = 3$ donors) in three separate experiments in triplicate. Error bars represent standard deviation between samples. Significance was determined using one-way analysis of variance (ANOVA) and Newman–Keuls test and is as compared to media sample; $^{***}P \leq 0{\cdot}001$.

and popular means to monitor lymphocyte division [28]. CFSE-labelled CD3$^+$CD56$^-$ T lymphocytes were co-cultured with or without freshly isolated unlabelled autologous CD56^{dim} or CD56^{bright} NK subsets (cell purities were routinely ≥ 97%). NK cells comprise approximately 10% of circulating lymphocytes in humans and 90% of peripheral blood; spleen NK cells belong to the CD56^{dim} and 10% belong to the CD56^{bright} NK subset [10,11,13,29]. For these experiments, we therefore cultured the CFSE-incorporated T cells with cells at a ratio of 1 : 100 CD56^{bright} NK cells to T cells and CD56^{dim} NK cells at a ratio of 1 : 10 CD56^{dim} NK cells to T cells, which mimics the peripheral physiological ratios of these cells *in vivo*. Purified CD3$^+$ T cell proliferation contracted significantly at low and high IL-2 concentrations when CD56^{bright} NK cells were present (Fig. 3a–d). While there was a slight overall drop in proliferation (corresponding to increased p27 in the previous experiment) when CD56^{dim} NK cells were added, this was insignificant and not dependent on IL-2 concentrations (Fig. 3a–d). To investigate the effect of IL-2 on NK cell proliferation a reciprocal experiment was performed whereby the CD56^{dim} and CD56^{bright} subsets were CFSE-labelled and co-cultured with unlabelled autologous CD3$^+$CD56$^-$ T cells. This assessment of NK cell subset proliferation in response to IL-2 found that CD56^{bright} NK cells undergo

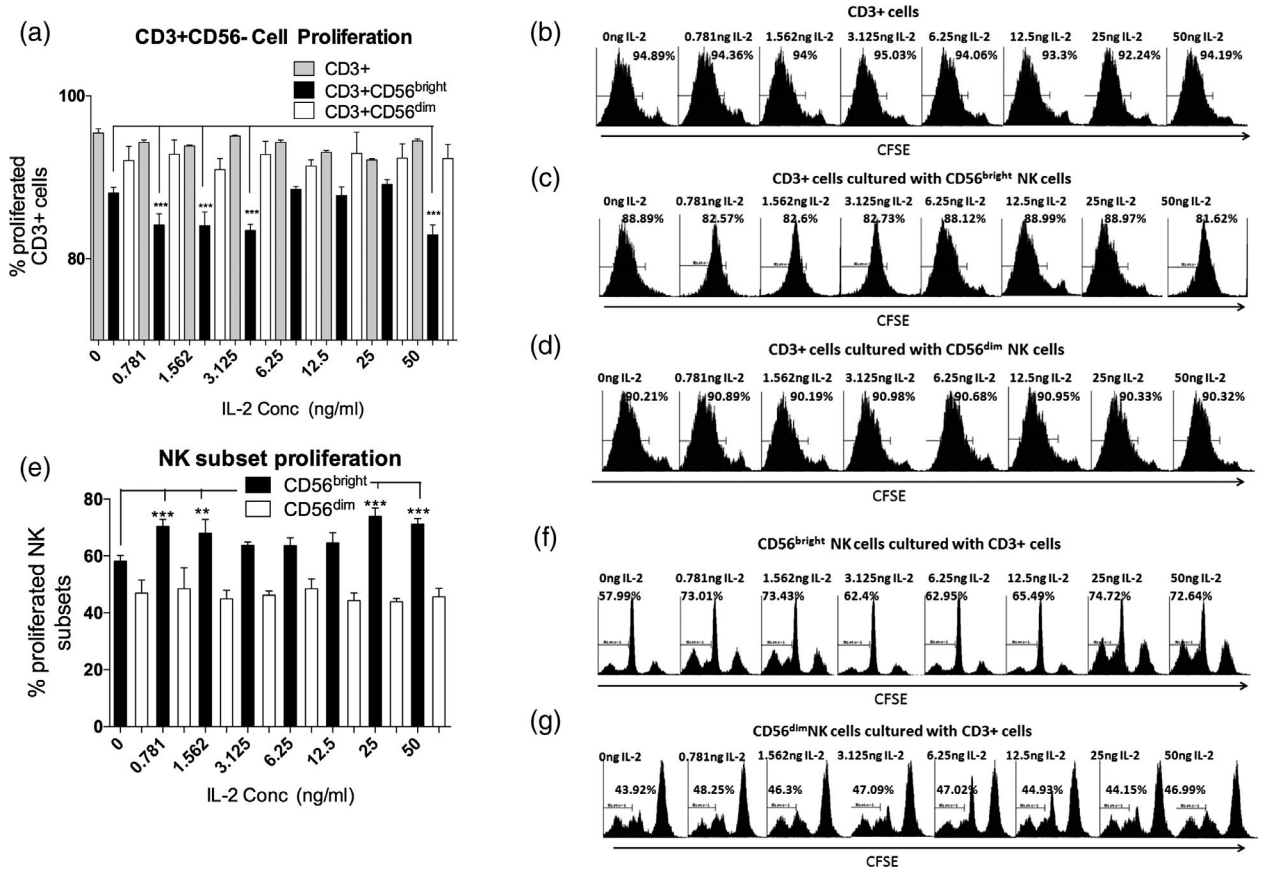

Fig. 3. Natural killer (NK) cell inhibit proliferation of CD3$^+$ cells and the regulation is mediated by the CD56^{bright} NK subset. (a–d) CD3$^+$ cells [isolated from peripheral blood mononuclear cells (PBMCs)] were carboxyfluorescein succinimidyl ester (CFSE)-labelled and cultured alone or in co-culture with CD56^{bright} or CD56^{dim} NK cells and stimulated with increasing IL-2 (0–50 ng). After 5 days, CD3$^+$ proliferative responses (cultured alone or in co-culture with NK cell subsets) were revealed by determining the percentage of low CFSE (or proliferated) cells by flow cytometry. (a) Bar charts represent normalized proliferative data for CD3$^+$ cells (n = 3 donors), with each donor experiment carried out in triplicate. Values are expressed as percentage + standard error of the mean (s.e.m.). (b–d) Representative histogram plots for CFSE fluorescence at the low and high-doses of IL-2 for one donor (of n = 3), with the percentage of low CFSE cells indicated within the plot. (e–g) Similarly, in a separate experiment for the same donors, isolated CD56^{bright} or CD56^{dim} NK cells were CFSE incorporated prior to IL-2 stimulation and co-cultured with unlabelled CD3$^+$ cells. After 5 days, the percentage of proliferated cells for each cell type was determined (low CFSE). (e) Bar charts represent normalized proliferative data for NK cell subsets (n = 3 donors), with each donor experiment carried out in triplicate. Values are expressed as percentage mean + standard error of the mean (s.e.m.). (f,g) Representative CFSE histograms at the low and high-doses of IL-2 for one donor (from n = 3) for NK cell subsets co-cultured with CD3$^+$ cells. The percentage of low CFSE cells is indicated within each plot. For normalized data, significance was determined using one-way analysis of variance (ANOVA) and Newman–Keuls test and is as compared to the media sample of same data set; $^{**}P \leq 0{\cdot}01$, $^{***}P \leq 0{\cdot}001$.

proliferation at low and high IL-2 concentrations (Fig. 3e–g). However, CD56^{dim} NK cell proliferation was unaffected by IL-2 stimulation and remained relatively constant for each dose of IL-2 (Fig. 3e–g). These results imply that NK cells reduce the overall proliferation of CD3$^+$CD56$^-$ T cells and the CD56^{bright} subset of NK cells is responsible for T cell regulation of expansion at low and high IL-2 levels.

The human IL-2 receptor exists as both an intermediate affinity receptor and a high-affinity receptor generated by different combinations of three different proteins, often referred to as 'chains': α (also called IL-2Rα or CD25), β (also called IL-2Rβ, p75 or CD122) and γ (also called IL-2Rγ, γc, common gamma chain or CD132) The combination of β and γ together form a complex that binds IL-2 with intermediate affinity, and all three receptor chains form a complex that binds IL-2 with high affinity on activated T cells and T_{regs} [30]. Based on analysis of more than 20 normal donors, an early study has demonstrated that both CD16$^-$CD56^{bright} and CD16$^+$CD56^{dim} NK cell subsets expressed the IL-2Rβ (p75, CD122); however, only the CD16$^-$CD56^{bright} NK cells constitutively expressed detectable IL-2Rα (CD25) [31]. We sought to determine which receptor is primarily involved in capturing the signal to induce NK regulation of T cell proliferation. Results demonstrate that blocking the IL-2Rα on NK cells did not impact upon the NK regulation of T cell proliferation at low- and high-dose IL-2; however, blocking IL-2Rβ chain of the intermediate receptor on NK cells alone or in combination with the IL-2Rα chain restored the proliferation status of the CD3$^+$CD56$^-$ in response to IL-2 (Fig. 4a). This finding is supported by other studies in humans whereby CD25 (IL-2Rα) antagonism has been shown *in vitro* to increase IL-2 availability and intermediate-affinity IL-2 signalling in CD56^{bright} NK cells. Moreover, intermediate-affinity IL-2 receptor (IL-2Rβ) expression predicts CD56^{bright} NK cell expansion after anti IL-2Rα treatment in patients with MS [32,33].

To establish if direct contact with the CD3$^+$ T cells is required, we performed Transwell studies on a further three human donors. For this experiment, we again assessed the level of T cell cycling and apoptosis at various IL-2 concentrations in purified CD3$^+$ and purified CD3$^-$CD56$^+$ NK cells together or separated by 0·2 μm pore insert. The latter allows movement of soluble factors such as cytokines, but prevents contact between the NK and T cells. Both NK-dependent cell cycle arrest at low-dose IL-2 and apoptosis at high-dose IL-2 were abrogated when direct contact between these cell groups was prevented (Fig. 5a,b). This suggested that NK surface receptors may be responsible for the regulation of T cell proliferation. In our previous studies with HPIV3, we found that blocking NKp44 and NKp46 was sufficient to block the CD56

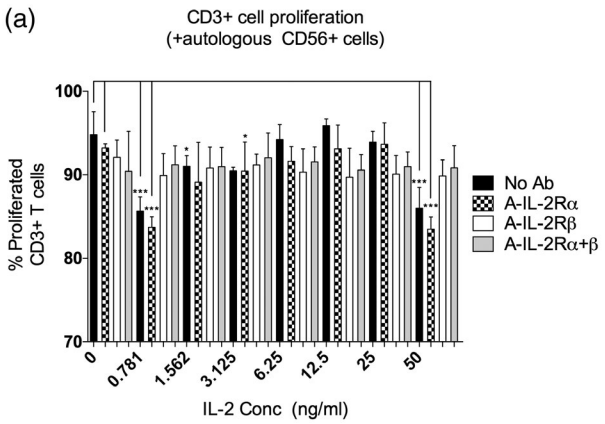

Fig. 4. Natural killer (NK) cells respond via the intermediate-affinity and not the high-affinity interleukin (IL)-2 receptor to exert regulation of CD3$^+$ T cell proliferation. (a) Proliferative responses of CD3$^+$ cells cultured with CD56$^+$ cells with blocked IL-2R components were examined. Both CD56$^+$ and CD3$^+$ cells were isolated from freshly cultured peripheral blood mononuclear cells (PBMCs). Carboxyfluorescein succinimidyl ester (CFSE) was incorporated into CD3$^+$ cells only. Receptor-specific antibodies were used to block IL-2Rα, IL-2Rβ or both receptors (or neither when no antibody was used) on CD56$^+$ cells prior to co-culture and IL-2 stimulation for 5 days. Cells were analysed for CFSE intensity and cells in the 'low CFSE' peak of the acquired histogram were gated and plotted as a percentage of total CFSE$^+$ cells. Results represent normalized data (n = 3 donors). Error bars represent standard deviation + standard error of the mean (s.e.m.). Significance was determined using one-way analysis of variance (ANOVA) with Newman–Keuls test and is as compared to media samples of the same data set; $^*P \leq 0{\cdot}05$, $^{***}P \leq 0{\cdot}001$.

NK^{bright}-dependent inhibition of T cell proliferation by HPIV3 [25]. Other studies also demonstrated that blocking the human NK receptors NKp44 or NKp46 was sufficient to abrogate increased human NK binding to cells in mitotic division [34]. We hypothesized that NKp44 and NKp46 may be involved in the NK regulation of cell cycle in response to IL-2 levels. Experiments showed that blocking NKp46 resulted in a loss of cell cycle arrest at the lowest doses and apoptosis at the second highest dose of IL-2, but apoptosis continued in the highest dose (Fig. 5c,d and Supporting information, Fig. 1A–H). Blocking NKp44 resulted in both a loss of NK cell cycle control at low IL-2 and apoptosis at both high doses of IL-2, with no effects observed with either antibodies blocking NKp30 and no antibody controls (Fig. 5c,d and Supporting information, Fig. 1A–H). We examined the expression of these receptors in response to IL-2 and found that both receptors are increased at low IL-2, but NKp44 appears to predominate at high-dose IL-2 (Supporting information, Fig. 2), explaining why blocking NKp46 did not have any real effect at the highest dose of IL-2. These findings suggest that it is the relative expression of NKp44 to

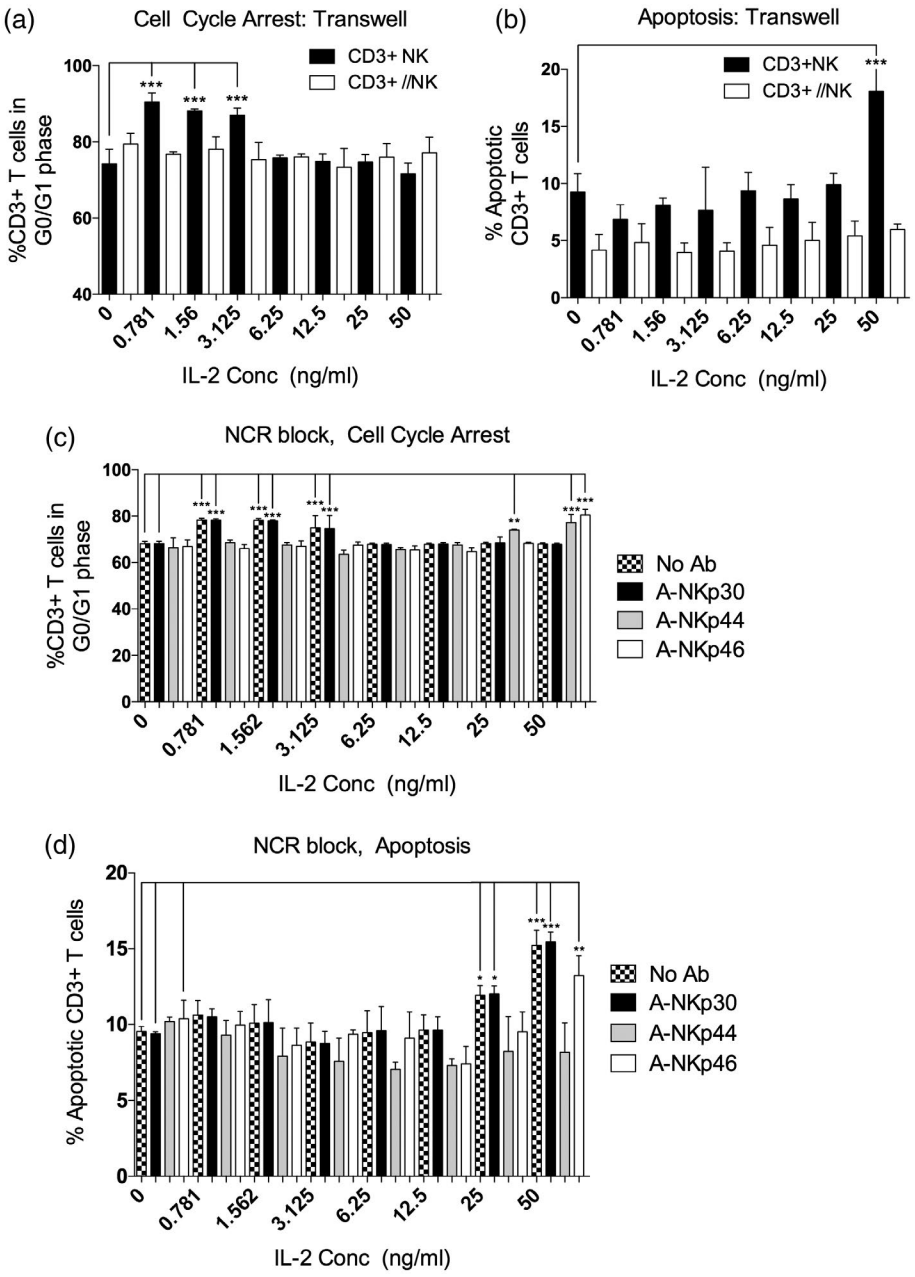

Fig. 5. Natural killer (NK) regulation of CD3$^+$ T cell expansion is contact-dependent; blocking NKp44 and NKp46 restores the cell cycle at low interleukin (IL)-2 and prevents apoptosis at high IL-2. (a,b) Cell cycle and apoptotic responses of CD3$^+$ cells in response to IL-2 when cultured with NK cells in contact (CD3$^+$ NK) or without contact (CD3$^+$/NK) (Transwell). Both CD56$^+$ and CD3$^+$ cells were isolated from freshly cultured peripheral blood mononuclear cells (PBMCs) before co-culture with or without contact and then stimulated with increasing IL-2 (0–50 ng) for 5 days. Cells were then stained with an allophycocyanin (APC)-labelled anti-CD3 antibody. (a) Cell cycle status was determined for CD3$^+$ cells by propidium iodide (PI) staining and flow cytometry. The percentage of CD3$^+$ in the G0/G1 phase was determined. (b) Apoptosis was assessed by PI and annexin V staining for CD3$^+$ cells. The percentage of apoptotic CD3$^+$ cells was determined. (c,d) Cell cycle and apoptotic responses of CD3$^+$ cells in a mixed lymphocyte (ML) population in response to IL-2 when cultured either without antibody or pretreated with blocking antibodies A-NKp30, A-NKp44 or A-NKp46. MLs were cultured with or without the blocking antibodies A-Np30, A-NKp44 or A-NKp46, and then stimulated with IL-2 (0–50 ng) and cultured for 5 days. Cells were then stained with APC-labelled anti-CD3 antibody. (c) Cell cycle status was determined for CD3$^+$ cells by PI staining and flow cytometry. The percentage of CD3$^+$ in the G0/G1 phase was determined. (d) Apoptosis was assessed by PI and annexin V staining for CD3$^+$ cells. The percentage of apoptotic CD3$^+$ cells was determined. Bar charts for cell cycle and apoptotic analysis represent normalized data (n = 3 donors). Values are expressed as percentage + standard error of the mean (s.e.m.). Significance was determined using one-way analysis of variance (ANOVA) with Newman–Keuls test and is as compared to the media sample of the same data set; $^*P \leq 0{\cdot}05$, $^{**}P \leq 0{\cdot}01$, $^{***}P \leq 0{\cdot}001$.

NKp46 that may dictate the cell fate regulation mechanism of the NK cells (Supporting information, Fig. 3). These results suggest that low IL-2 activates NK cells via NKp44 and NKp46 to induce T cell cycle arrest, while high IL-2 activates NK cell-mediated T cell apoptosis via elevated levels of NKp44.

Having demonstrated that NK cells inhibit the overall $CD3^+$ population at low and high IL-2, we sought to investigate the effect of NK cells on specific key populations of T cells in response to IL-2. In keeping with the beneficial effects of low-dose IL-2 treatment in humans, we found that the percentage of cells expressing key pro-inflammatory T cell subset markers are reduced at low IL-2 in the presence of NK cells, but again we observed an increase in these cell subsets when $CD56^+$ NK cells were depleted from the lymphocyte cultures. The proportion of both Th1 and Th17 cells and $CD8^+$ cells were significantly reduced in the presence of NK cells at low and high IL-2, supporting a beneficial role for these cells in IL-2-based treatment modalities (Fig. 6a–c). Additionally, the percentage of CD45RO-expressing $CD3^+$ T cells is decreased, although not significantly, in the presence of NK cells at low and high IL-2 (Fig. 6d). Conversely to the overall T cell population, the presence of NK cells actually boosted the percentage of cells expressing T_{reg} markers in ML populations at low doses of IL-2 (Fig. 6e).

To ascertain if the enhancement of the percentage of cells expressing T_{reg} markers corresponds to proliferation of the T_{reg} population, and to characterize the involvement of $CD56^{bright}$ NK cells, we isolated T_{reg} populations ($CD4^+CD25^+$) and $CD56^{bright}$NK cells ($CD56^+CD16^-$) and examined T_{reg} proliferation with or without $CD56^{bright}$ NK cells in response to IL-2 by CFSE incorporation. Strikingly, isolated T_{regs} proliferated poorly to IL-2 in the absence of $CD56^+$ NK cells and demonstrated a significant increase in proliferation when purified $CD56^{bright}$ NK were added to the cultures (Fig. 7a). The increase in T_{regs} was more pronounced at low and high IL-2 in the presence of $CD56^{bright}$NK regulators. To establish if the increase in T_{regs} was involved in the regulation of T_{eff} cell proliferation by NKs we depleted the T_{regs} from the $CD3^+$ cells and assessed the proliferation of these CFSE-incorporated remaining T cells in the presence or absence of purified $CD56^+$ and NK cells in a further three donors. $CD56^+$ NK cells continued to regulate proliferation in T_{reg}-depleted cultures, which remained more pronounced at low- and high-dose IL-2 (Fig. 7b).

Discussion

Low-dose IL-2 has been administered to humans in a number of settings including inflammatory disorders, infection, cancer and healthy volunteers [1–4,35–38]. Without exception, these studies report an increase in NK cells in response to this cytokine in humans. T_{regs} also increase in mice and humans in response to this treatment and a role for T_{regs} in the beneficial effects of low-dose IL-2 in autoimmune conditions has been established.

Our group has demonstrated that HPIV3-infected human dendritic cells (DCs) could drive $CD56^+$ NK cell regulation of human T cell proliferation. This regulation was associated with low IL-2 levels, and additional IL-2 could restore the anti-proliferative regulation [24]. This led us to speculate that low-dose IL-2 may target similar pathways to HPIV3 to contract T_{eff} cells. Several reports have revealed that high IL-2 availability may induce NK cells to kill autologous T cells [16,32,39–42].

Here, we demonstrate that *in-vitro* human $CD56^{bright}$ NK cells exhibit dual regulation of T cell proliferation in response to IL-2, which may explain some of the diverse reports relating to these cells. We demonstrate that NK cells regulate T cells by two different mechanisms, depending on the level of IL-2 in the milieu. At low doses of IL-2, $CD56^{bright}$ NK regulate by a cell cycle arrest mechanism, and at high IL-2 these cells become cytotoxic towards autologous T cells. Furthermore, we present data from a further set of donors demonstrating that NK cells respond to low-dose IL-2 by driving retention of the cell cycle inhibitor p21 in arrested cells. We also show that increased cytotoxicity is consistent with increasing levels of perforin in NK cells in response to IL-2. Interestingly, it is the intermediate affinity receptor IL-2Rβ on the NK cells that mediates this response to low- and high-dose IL-2. In addition, recent reports have suggested an association with single nucleotide polymorphisms in the IL-2Rβ gene in autoimmune conditions such as RA, myasthenia gravis (MG), asthma and TID [43–45]. Moreover, reports from patients receiving a blocking antibody to IL-2Rα confirms that, in these patients, IL-2 signals through the IL-2β receptor, resulting in the expansion of $CD56^{bright}$ NK cells *in vivo* and improved clinical outcomes [33].

In addition, we confirm in our *in-vitro* primary human cultures that the $CD56^{bright}$ NK cell subset expands in response to low-dose IL-2 and is responsible for inhibited T cell proliferation at low and high doses of this cytokine. The threat of inflammation is inherently linked to cell cycle progression of T_{effs} coupled by a decrease in T_{regs} leading to an imbalance of activation and regulation. An early report has demonstrated that human NKs can recognize and bind to autologous cells in mitosis [34]. Recognition is mediated via ligation of activating receptors binding to target cell hyaluronan, a component of the pericellular matrix known to be increased during mitosis. The key activating receptors identified in this report were the NCR NKp44 and NKp46, and coincidentally HPIV3 surface glycoproteins HN bind to these receptors in humans

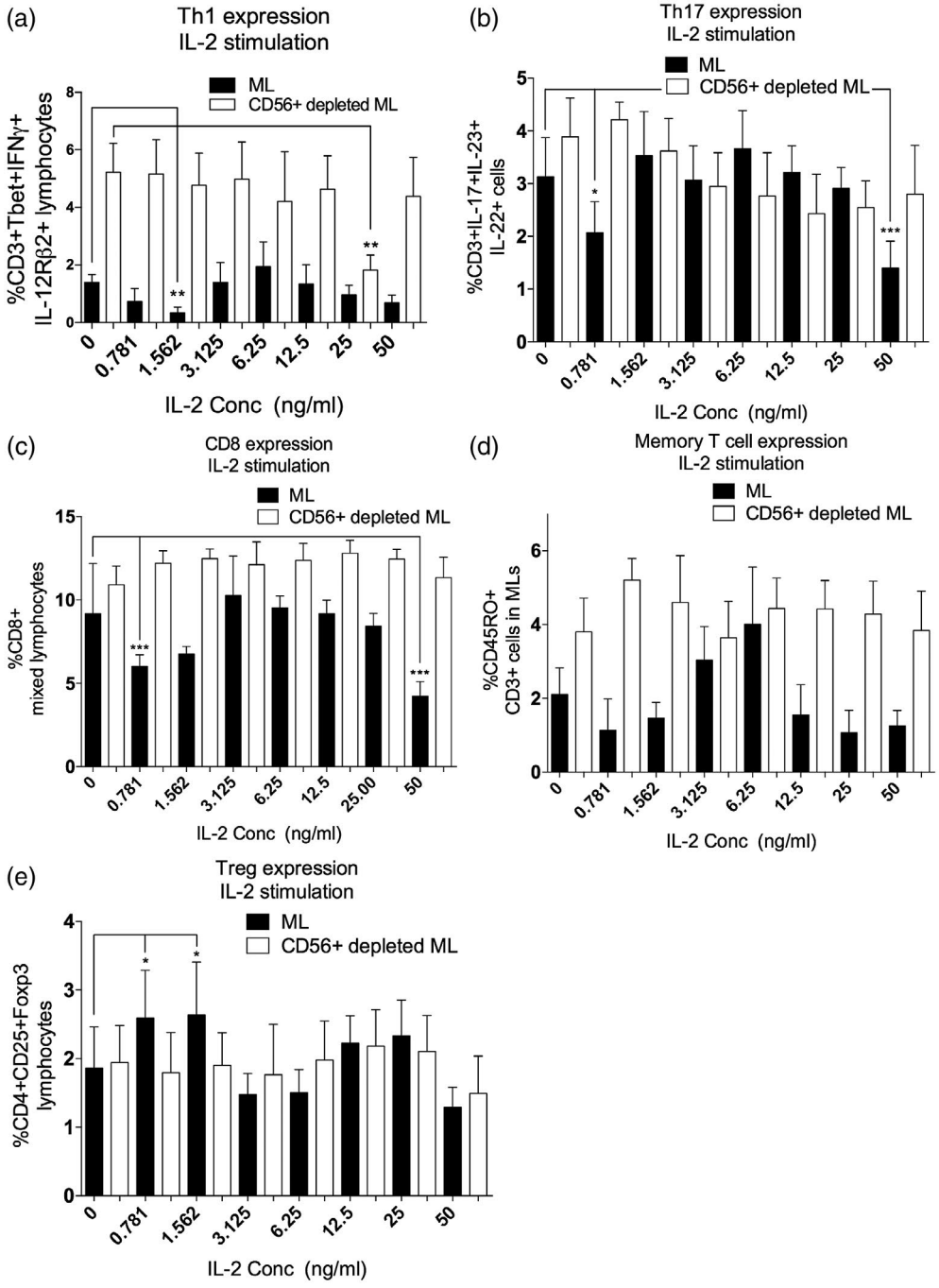

Fig. 6. CD56$^+$ Natural killer (NK) enhanced cells expressing regulatory T cell (T_{reg}) markers while continuing to inhibit cells expressing conventional T cell markers within lymphocyte cultures. Mixed lymphocytes (MLs) and CD56$^+$ cell-depleted MLs were isolated from freshly cultured peripheral blood mononuclear cells (PBMCs), stimulated with increasing concentrations of interleukin (IL)-2 (0–50 ng) and cultured for 5 days. Cells were stained for T cell subset markers as follows: CD3$^+$Tbet$^+$interferon (IFN)-γ$^+$IL-12Rβ2$^+$ represent T helper type 1 (Th1) cells (a), CD2$^+$IL-17$^+$IL-23$^+$IL-22$^+$ represent Th17 cells (b), CD3$^+$CD8$^+$ cells represent CD8$^+$ T cells (c), CD3$^+$CD45RO$^+$ cells represent memory T cells (d) and CD4$^+$CD25$^+$forkhead box protein 3 (FoxP3)$^+$ cells represent T_{regs} (e). Upon acquisition and gating, each subset was expressed and plotted as a percentage of total MLs. Results represent normalized data (n = 3 donors) in triplicate. Values are expressed as percentage + standard error of the mean (s.e.m.). Significance was determined using one-way analysis of variance (ANOVA) with Newman–Keuls test and is as compared to the media sample of the same data set; $^*P \leq 0{\cdot}05$, $^{**}P \leq 0{\cdot}01$, $^{***}P \leq 0{\cdot}001$.

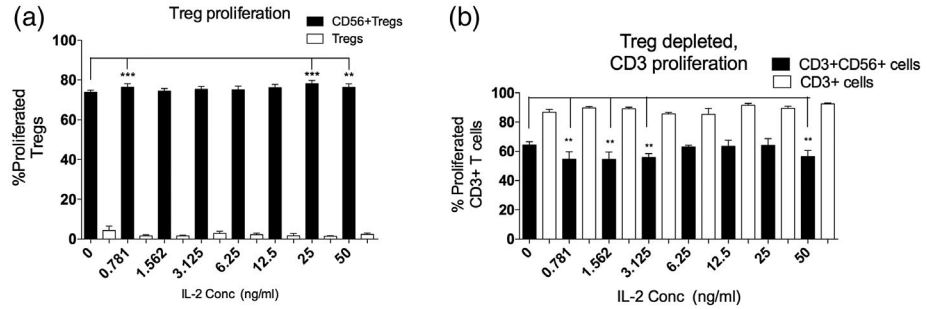

Fig. 7. The presence of CD56 natural killer (NK)$^+$ cells increases proliferation of regulatory T cells (T_{regs}) and T_{reg} depletion did not affect NK regulation of T effector cell proliferation. (a) T_{regs} and CD56$^+$ cells were isolated from freshly cultured peripheral blood mononuclear cells (PBMCs). Carboxyfluorescein succinimidyl ester (CFSE) was incorporated into T_{regs}, which were cultured alone or with CD56$^+$ cells, and stimulated with increasing interleukin (IL-2) (0–50 ng) for 5 days. CFSE intensity was determined by flow cytometry. Cells in the 'low CFSE peak' of the acquired histogram were gated and plotted as a percentage of total T_{regs}. Bar chart represents normalized data (n = 3 donors), with experiments carried out in triplicate. (b) T_{reg}-depleted CD3$^+$ cells (CD3$^+$$T_{reg}^-$) and CD56$^+$ cells were isolated from PBMCs. CFSE was incorporated into CD3$^+$$T_{reg}^-$ cells which were cultured alone or with CD56$^+$ cells. Cultures were stimulated with increasing IL-2 (0–50 ng) for 5 days. CFSE intensity was determined by flow cytometry. Cells in the 'low CFSE peak' of the acquired histogram were gated and plotted as a percentage of total CD3$^+$$T_{reg}^-$ cells. Bar chart represents normalized data (n = 3 donors), with experiments carried out in triplicate. Values are expressed as percentage + standard error of the mean (s.e.m.). Significance was determined using one-way analysis of variance (ANOVA) with Newman–Keuls test and is as compared to the media sample of the same data set; $^{**}P \leq 0{\cdot}01$, $^{***}P \leq 0{\cdot}001$.

[34,46–48]. In keeping with this study and our data with HPIV3, we find that human NK cells require contact with the CD3$^+$ T cells and NCR receptors NKp44 and NKp46 availability is necessary for cell cycle arrest at low-dose IL-2. Blocking both NKp44 and NKp46 resulted in loss of cell cycle arrest of T cells by NKs at low-dose IL-2. The involvement of NKp44 in this human NK regulation of T cell expansion in response to IL-2 therapy, if observed *in vivo* in humans, is noteworthy. Studies of this receptor suggest that it is a human NCR which only recently emerged in speciation, acquiring functional relevance only in non-human primates closest to *Homo sapiens* [46,49]. Therefore, this aspect of human immune regulation is unlikely to be identified in animal models of disease. Indeed, the reduced expansion of NK cells in cynomolgus monkeys compared to humans was considered a modelling limitation by authors in a recent study investigating the immune response to ultra-low doses of IL-2 fusion protein [50].

From our *in-vitro* study, human NK cells proliferate at low- and high-dose IL-2 and regulate expansion of CD3$^+$ T cells via NCRs NKp44 and NKp46. These results suggest a control mechanism which ensures that a threshold of activation must be achieved before T cell proliferation is permitted by NK cell regulators. Similarly, cytotoxicity by apoptosis represents a more suitable control when activation (IL-2 levels) has reached the upper limit, and elimination of offending cells is key to regaining intermediate or low levels of immune activity. As an increase in T_{regs} has also been consistently reported following low-dose IL-2 therapy, we sought to investigate if NK cells are selective in the T cell subsets they regulate in response to IL-2. We found a marked reduction in key proinflammatory cell subsets such as Th1 and Th17 when NK cells were present, and these were significantly reduced at low IL-2 for both subsets and Th17 at high IL-2. Moreover, CD8 and memory expression followed similar profiles. Conversely, the presence of NKs resulted in an increase in cells expressing T_{reg} markers at low-dose IL-2. Further examination of the effect of NKs on the proliferation of T_{regs} demonstrated that T_{regs} proliferate strongly in the presence of CD56^{bright} NK cells, which is more elevated at low- and high-dose IL-2.

To assess if the T_{reg} population within the lymphocyte populations has a bearing on NK regulation of T_{effs}, we depleted the T_{reg} population from the cultures and found no difference in the contraction of the lymphocytes at low and high IL-2 in the presence of NK cells. Again, with this set of donors we find that the presence of NKs lowers the overall proliferation of the lymphocyte population and this corresponds to the cell cycle inhibitor profile detected in earlier experiments. From these data it appears that, at least *in vitro*, primary human NK cells may directly contract T_{effs} at low- and high-dose IL-2 but that they may also enhance the levels of T_{regs} in response to this cytokine. Variation exists in the reporting of the increase in NK cells and T_{regs} at low and ultra-low doses of IL-2. In our *in-vitro* study, the mechanism of NK regulation of T_{eff} proliferation is clear and mediated by NCRs; however, the mechanism of T_{reg} enhancement by NK cells is less so. There are a number of studies suggesting that T_{regs} influence NK function in humans and animals but sparse information from the literature on the influence of NKs on T_{reg} proliferation or function [42,51,52]. We also observe in our studies from a further set of donors that human allogeneic NK cells also induce regulation of T cell proliferation at

low- and high-dose IL-2 in a similar manner to autologous NK cells (Supporting information, Fig. 4).

We demonstrate that NK cells exhibit a dual mechanism of cell cycle arrest at low-dose IL-2 and cytotoxicity at high-dose IL-2. High-dose IL-2 has been used in the treatment of certain cancers with limited efficacy. Increased T_{reg} levels and the development of somewhat lethal toxicity was considered a major limitation to this intervention [53]. These results are in line with our findings, which suggest that that NK cells regulate T_{regs} in response to IL-2 at low and high doses. Further knowledge on how NK T_{regs} respond to IL-2 may provide another avenue to harness the anti-tumour responses to this cytokine while limiting immunosuppression. In addition, our results would suggest that where immune activation and anti-tumour effects are sought neither low- or high-dose IL-2 will prove beneficial and that an optimal medium to high dose may prove more effective.

Further investigations, especially involving reciprocal NK/T_{reg} cross-talk, are necessary to delineate the regulatory mechanisms and to establish if these *in-vitro* primary human responses to IL-2 are relevant to the *in-vivo* responses in humans. The expansion and activation of T_{regs} either *in vivo* or *in vitro* for therapeutic infusion represents a very promising approach to the treatment of autoimmune disorders; therefore, establishing a role for NKs in T_{reg} expansion must have a significant impact on the therapeutic exploitation of this regulatory arm of human immunity. Overall, these findings present a novel mechanism of NK regulation and supports a beneficial role for CD56^{bright} NK in IL-2-associated therapies in humans.

Acknowledgements

This work was funded by the Irish Health Research Board grant ref: HRA/2009/128 awarded to P. A. J.

Disclosures

The authors have declared that no conflicts of interest exist.

References

1 Koreth J, Matsuoka K, Kim HT *et al*. Interleukin-2 and regulatory T cells in graft-versus-host disease. N Engl J Med 2011; **365**:2055–66.

2 Saadoun D, Rosenzwajg M, Joly F *et al*. Regulatory T-cell responses to low-dose interleukin-2 in HCV-induced vasculitis. N Engl J Med 2011; **365**:2067–77.

3 Hartemann A, Bensimon G, Payan CA *et al*. Low-dose interleukin 2 in patients with type 1 diabetes: a phase 1/2 randomised, double-blind, placebo-controlled trial. Lancet Diabetes Endocrinol 2013; **1**:295–305.

4 Long SA, Rieck M, Sanda S *et al*. Rapamycin/IL-2 combination therapy in patients with type 1 diabetes augments Treg yet transiently impairs beta-cell function. Diabetes 2012; **61**:2340–8.

5 Kosmaczewska A. Low-dose interleukin-2 therapy: a driver of an imbalance between immune tolerance and autoimmunity. Int J Mol Sci 2014; **15**:18574–92.

6 Setoguchi R, Hori S, Takahashi T, Sakaguchi S. Homeostatic maintenance of natural Foxp3+CD25+CD4+ regulatory T cells by interleukin (IL)-2 and induction of autoimmune disease by IL-2 neutralization. J Exp Med 2005; **201**:723–35.

7 Grinberg-Bleyer Y, Baeyens A, You S *et al*. IL-2 reverses established type 1 diabetes in NOD mice by a local effect on pancreatic regulatory T cells. J Exp Med 2010; **207**:1871–8.

8 Dinh TN, Kyaw TS, Kanellakis P *et al*. Cytokine therapy with interleukin-2/anti-interleukin-2 monoclonal antibody complexes expands CD4+CD25+Foxp3+ regulatory T cells and attenuates development and progression of atherosclerosis. Circulation 2012; **126**:1256–66.

9 Matsuoka K, Koreth J, Kim HT *et al*. Low-dose interleukin-2 therapy restores regulatory T cell homeostasis in patients with chronic graft-versus-host disease. Sci Transl Med 2013; **5**:179ra43.

10 Caligiuri MA. Human natural killer cells. Blood 2008; **112**:461–9.

11 Shereck E, Satwani P, Morris E, Cairo MS. Human natural killer cells in health and disease. Pediatr Blood Cancer 2007; **49**:615–23.

12 Poznanski SM, Ashkar AA. What defines NK cell functional fate: phenotype or metabolism? Front Immunol 2019; **10**:1414.

13 Bielekova B, Catalfamo M, Reichert-Scrivner S *et al*. Regulatory CD56^{bright} natural killer cells mediate immunomodulatory effects of IL-2Rα-targeted therapy (daclizumab) in multiple sclerosis. Proc Natl Acad Sci USA 2006; **103**:5941–6.

14 Ullrich E, Salzmann-Manrique E, Bakhtiar S *et al*. Relation between acute GVHD and NK cell subset reconstitution following allogeneic stem cell transplantation. Front Immunol 2016; **7**:595.

15 Chang YJ, Zhao XY, Huang XJ. Effects of the NK cell recovery on outcomes of unmanipulated haploidentical blood and marrow transplantation for patients with hematologic malignancies. Biol Blood Marrow Transplant 2008; **14**:23–34.

16 Iniesta P, Revilla N, Chen-Liang TH *et al*. An early increase of CD56^{bright} natural killer subset as dominant effect and predictor of response to extracorporeal photopheresis for graft-versus-host disease. Transfusion 2018; **58**:2924–32.

17 Locatelli F, Moretta F, Brescia L, Merli P. Natural killer cells in the treatment of high-risk acute leukaemia. Semin Immunol 2014; **26**:173–9.

18 Kariminia A, Holtan SG, Ivison S *et al*. Heterogeneity of chromic graft-versus host disease biomarkers: association with CXCL10 and CXCR3+ NK cells. Blood 2016; **127**:3082–91.

19 Belizaire R, Kim HT, Poryanda SJ *et al*. Efficacy and immunologic effects of extracorporeal photopheresis plus interleukin-2 in chronic graft-versus-host disease. Blood Adv 2019; **3**:969–79.

20 Ni M, Wang L, Yang M *et al*. Shaping of CD56^{bright} natural killer cells in patients with steroid-refractory/resistant acute

graft-vs.-host disease via extracorporeal photopheresis. Front Immunol 2019; **10**:547.

21 Kastrukoff LF, Lau A, Wee R, Zecchini D, White R, Paty DW. Clinical relapses of multiple sclerosis are associated with 'novel' valleys in natural killer cell functional activity. J Neuroimmunol 2003; **145**:103–14.

22 Shibatomi K, Ida H, Yamasaki S *et al*. A novel role for interleukin-18 in human natural killer cell death: high serum levels and low natural killer cell numbers in patients with systemic autoimmune diseases. Arthritis Rheum 2001; **44**:884–92.

23 Lünemann A, Lünemann JD, Münz C. Regulatory NK-cell functions in inflammation and autoimmunity. Mol Med 2009; **15**:352–8.

24 Noone CM, Paget E, Lewis EA, Loetscher MR, Newman RW, Johnson PA. Natural killer cells regulate T-cell proliferation during human parainfluenza virus type 3 infection. J Virol 2008; **82**:9299–302.

25 McQuaid S, Loughran S, Power P *et al*. Haemagglutinin-neuraminidase from HPIV3 mediates human NK regulation of T cell proliferation via NKp44 and NKp46. J Gen Virol 2018; **99**:763–7.

26 Coqueret O. New roles for p21 and p27 cell-cycle inhibitors: a function for each cell compartment? Trends Cell Biol 2003; **13**:65–70.

27 Trapani JA, Smyth MJ. Functional significance of the perforin/granzyme cell death pathway. Nat Rev Immunol 2002; **2**:735–47.

28 Quah BJ, Parish CR. The use of carboxyfluorescein diacetate succinimidyl ester (CFSE) to monitor lymphocyte proliferation. J Vis Exp 2010; **44**:pii:2259.

29 Saraste M, Irjala H, Airas L. Expansion of $CD56^{bright}$natural killer cells in the peripheral blood of multiple sclerosis patients treated with interferon-beta. Neurol Sci 2007; **28**:121–6.

30 Malek TR, Castro I. Interleukin-2 receptor signaling: at the interface between tolerance and immunity. Immunity 2010; **33**:153–65.

31 Nagler A, Lanier LL, Phillips JH. Constitutive expression of high affinity interleukin 2 receptors on human CD16-natural killer cells *in vivo*. J Exp Med 1990; **171**:1527–33.

32 Martin JF, Perry JS, Jakhete NR, Wang X, Bielekova B. An IL-2 paradox: blocking CD25 on T cells induces IL-2-driven activation of CD56bright NK cells. J Immunol 2010; **185**:1311–20.

33 Sheridan JP, Zhang Y, Riester K *et al*. Intermediate-affinity interleukin-2 receptor expression predicts CD56(bright) natural killer cell expansion after daclizumab treatment in the choice study of patients with multiple sclerosis. Mult Scler 2011; **17**:1441–8.

34 Nolte-'t Hoen EN, Almeida CR, Cohen NR, Nedvetzki S, Yarwood H, Davis DM. Increased surveillance of cells in mitosis by human NK cells suggests a novel strategy for limiting tumor growth and viral replication. Blood 2007; **109**:670–3.

35 Khatri VP, Fehniger TA, Baiocchi RA *et al*. Ultra low dose interleukin-2 therapy promotes a type 1 cytokine profile in vivo in patients with AIDS and AIDS-associated malignancies. Clin Invest 1998; **101**:1373–8.

36 Bernstein ZP, Porter MM, Gould M *et al*. Prolonged administration of low-dose interleukin-2 in human immunodeficiency virus-associated malignancy results in selective expansion of innate immune effectors without significant clinical toxicity. Blood 1995; **86**:3287–94.

37 Meropol NJ, Porter M, Blumenson LE *et al*. Daily subcutaneous injection of low-dose interleukin 2 expands natural killer cells in vivo without significant toxicity. Clin Cancer Res 1996; **2**:669–77.

38 Fehniger TA, Bluman EM, Porter MM *et al*. Potential mechanisms of human natural killer cell expansion *in vivo* during low-dose IL-2 therapy. J Clin Invest 2000; **106**(1):117–24.

39 Harnack U, Johnen H, Percher G. Natural killer cell line YT exerts cytotoxicity against CD86 myeloma cells. Anticancer Res 2011; **31**:475–9.

40 Ren XB, Yu JP, Cao S *et al*. Antitumor effect of large doses IL-2-activated HLA haploidentical peripheral blood stem cells on refractory metastatic solid tumor treatment. Cancer Biother Radiopharm 2007; **22**:223–34.

41 Nielsen N, Ødum N, Ursø B, Lanier LL, Spee P. Cytotoxicity of CD56(bright) NK cells towards autologous activated CD4+ T cells is mediated through NKG2D, LFA-1 and TRAIL and dampened via CD94/NKG2A. PLOS ONE 2012; **7**:e31959.

42 Ralainirina N, Poli A, Michel T *et al*. Control of NK cell functions by CD4+CD25+ regulatory T cells. J Leukoc Biol 2007; **81**:144–53.

43 Ruyssen-Witrand A, Lukas C, Nigon D *et al*. Association of IL-2RA and IL-2RB genes with erosive status in early rheumatoid arthritis patients (ESPOIR and RMP cohorts). Joint Bone Spine 2014; **81**:228–34.

44 Pál Z, Antal P, Millinghoffer A *et al*. A novel galectin-1 and interleukin 2 receptor β haplotype is associated with autoimmune myasthenia gravis. J Neuroimmunol 2010; **229**:107–11.

45 Akhabir L, Sandford AJ. Genome-wide association studies for discovery of genes involved in asthma. Respirology 2011; **16**:396–406.

46 Biassoni R, Bottino C, Cantoni C, Moretta A. Human natural killer receptors and their ligands. Curr Protoc Immunol 2002; Unit 14:14.10.

47 Arnon TI, Lev M, Katz G, Chernobrov Y, Porgador A, Mandelboim O. Recognition of viral hemagglutinins by NKp44 but not by NKp30. Eur J Immunol 2001; **31**:2680–9.

48 Mandelboim O, Porgador A. NKp46. Int J Biochem Cell Biol 2001; **33**:1147–50.

49 De Maria A, Ugolotti E, Rutjens E *et al*. NKp44 expression, phylogenesis and function in non-human primate NK cells. Int Immunol 2009; **21**:245–55.

50 Bell CJ, Sun Y, Nowak UM *et al*. Sustained *in vivo* signaling by long-lived IL-2 induces prolonged increases of regulatory T cells. J Autoimmun 2015; **56**:66–80.

51 Bergmann C, Wild CA, Narwan M, Lotfi R, Lang S, Brandau S. Human tumor-induced and naturally occurring Treg cells differentially affect NK cells activated by either IL-2 or target cells. Eur J Immunol 2011; **41**:3564–73.

52 Zimmer J, Andres E, Hentges F. NK cells and Treg cells: a fascinating dance cheek to cheek. Eur J Immunol 2008; **38**:2942–5.

53 Choudhry H, Helmi N, Abdulaal WH *et al*. Prospects of IL-2 in cancer immunotherapy. Biomed Res Int 2018; **2018**:1–7.

Supporting Information

Additional supporting information may be found in the online version of this article at the publisher's web site:

Fig. S1. Blocking NKp44 and NKp46 restores cell cycle at low IL-2 and prevents apoptosis at high IL-2. (A-H) Cell cycle and apoptotic responses of CD3$^+$ cells in a ML population, in response to IL-2 concentrations, when cultured either without antibody, or pre-treated with blocking antibodies A-NKp30, A-NKp44 or A-NKp46. MLs were cultured with or without the blocking antibodies A-Np30, A-NKp44 or A-NKp46, and then stimulated with IL-2 (0-50 ng) concentrations and cultured for 5 days. Cells were then stained with an APC-labelled anti-CD3 antibody. (a-d) Cell cycle status was determined for CD3$^+$ cells by PI staining and flow cytometry. The percentage of CD3$^+$ in the G0/G1 phase was determined. Representative histograms for a single data set at the low and high doses of IL-2 for one donor (from $n = 3$ donors) are shown with the percentage of CD3+ in the G0/G1 phase indicated above each histogram. (e-h) Apoptosis was assessed by PI and Annexin V staining and flow cytometry for CD3$^+$ cells. Representative dot plots for a single data set at the low and high doses of IL-2 for one donor (from $n = 3$ donors) are shown with percentage of apoptotic CD3$^+$ cells (upper right quadrant) indicated above each dot plot.

Fig. S2. NKp44 and NKp30 receptors are increased at low IL-2 but NKp44 appears to predominate at high dose IL-2. (a,b) MLs were isolated from freshly cultured PBMCs and stimulated with increasing IL-2 (0-50 ng). After 5 days, cells were harvested, stained for CD56 and NCRs and analysed by flow cytometry. (a) The percentage of NCR expression on CD56+ cells was determined and plotted for each receptor. Bar chart represents normalized data ($n = 3$ donors), with experiments carried out in triplicate. Values are expressed as percentage mean +SEM. Significance was determined using one way ANOVA with Newman Keuls test and is as compared to the media sample of the same data set $^*P \leq 0.05$ $^{**}P \leq 0.01$ $^{***}P \leq 0.001$. (b) Representative histograms for a single data set at the low and high doses of IL-2 for one donor (from $n = 3$ donors) for each receptor are shown with the percentage NCR expression indicated above each histogram.

Fig. S3. Blocking NKp44 expression at high dose IL-2 is compensated for by up-regulation of NKp46. (a,b) MLs were isolated and cultured alone or with A-NKp44, before stimulation with increasing IL-2 (0-50 ng). After 5 days cells were stained for CD56 and NKp46 and analysed by flow cytometry. (a) The percentage of NKp46 expression on CD56$^+$ cells was determined and plotted. Bar chart represents normalized data ($n = 3$ donors), with experiments carried out in triplicate. Values are expressed as percentage mean +SEM. Significance was determined using one way ANOVA with Newman Keuls test and is as compared to the media sample of the same data set, $^*P \leq 0.05$, $^{***}P \leq 0.001$. (b) Representative histograms for a single data set at the low and high doses of IL-2 for one donor (from $n = 3$ donors) for the NKp46 receptor are shown with the percentage expression indicated above each histogram.

Fig. S4. Allogeneic NK cells induce regulation of T cell proliferation at low and high dose IL-2. (a,b) CD56$^+$ and CD3$^+$ cells were isolated from freshly cultured PBMCs from two separate donors. CFSE was incorporated into CD3$^+$ cells, which were cultured either alone, or cocultured with CD56$^+$ cells, and stimulated with increasing IL-2 (0-50 ng) for 5 days. CFSE intensity was determined by flow cytometry. (a) Cells in the "low CFSE peak" of the acquired histogram were gated and plotted as a percentage of total cells. Bar chart represents normalized data ($n = 3$ donors), with experiments carried out in triplicate. Values are expressed as percentage mean +SEM. Significance was determined using one way ANOVA with Newman Keuls test and is as compared to the media sample of the same data set, $^*P \leq 0.05$, $^{***}P \leq 0.001$. (b) Histograms for CFSE intensity represent a single data set at the low and high doses of IL-2 for one donor (of $n = 3$ above) with the percentage of cells in the "low-CFSE" gate displayed above each histogram.

Fig. S5. The proportion of both Th1 and Th17 cells is significantly reduced in the presence of NK cells at low and high IL-2. (a,b) MLs and CD56$^+$ cell depleted MLs were isolated from freshly cultured PBMCs, stimulated with increasing concentrations of IL-2 (0-50 ng) and cultured for 5 days. Cells were stained for T cell subset markers and representative histograms for a single data set at the low and high doses of IL-2 for one donor (from $n = 3$ donors) are shown for (a) Th1 cells (CD3$^+$Tbet$^+$IFN-γ^+IL-12Rβ2$^+$) and (b) Th17 cells (CD2$^+$IL-17$^+$IL-23$^+$IL-22$_+$) with the percentage expression indicated above each histogram.

Fig. S6. T cell subset expression in the presence of NK cells at low and high IL-2. (c-e) MLs and CD56$^+$ cell depleted MLs were isolated from freshly cultured PBMCs, stimulated with increasing concentrations of IL-2 (0-50 ng) and cultured for 5 days. Cells were stained for T cell subset markers and representative histograms for a single data set at the low and high doses of IL-2 for one donor (from $n = 3$ donors) are shown for (c) CD8$^+$ T cells (CD3$^+$CD8$^+$) and (d) memory T cells (CD3$^+$CD45RO$^+$) and (e) Tregs (CD4$^+$CD25$^+$FOXP3$^+$) with the percentage expression indicated above each histogram.